

# An Automated Dental Caries Detection and Scoring System for Optical Images of Tooth Occlusal Surface

Leila Ghaedi-*IEEE Student Member*, Riki Gottlieb, David C. Sarrett, Amid Ismail, Ashwin Belle-*IEEE Member*, Kayvan Najarian-*IEEE Senior Member* Rosalyn Hobson Hargraves-*IEEE Member*

**Abstract**— Dental caries are one of the most prevalent chronic diseases. The management of dental caries demands detection of carious lesions at early stages. This study aims to design an automated system to detect and score caries lesions based on optical images of the occlusal tooth surface according to the International Caries Detection and Assessment System (ICDAS) guidelines. The system detects the tooth boundaries and irregular regions, and extracts 77 features from each image. These features include statistical measures of color space, grayscale image, as well as Wavelet Transform and Fourier Transform based features. Used in this study were 88 occlusal surface photographs of extracted teeth examined and scored by ICDAS experts. Seven ICDAS codes which show the different stages in caries development were collapsed into three classes: score 0, scores 1 and 2, and scores 3 to 6. The system shows accuracy of 86.3%, specificity of 91.7%, and sensitivity of 83.0% in ten-fold cross validation in classification of the tooth images. While the system needs further improvement and validation using larger datasets, it presents promising potential for clinical diagnostics with high accuracy and minimal cost. This is a notable advantage over existing systems requiring expensive imaging and external hardware.

## I. INTRODUCTION

According to World Health Organization report on oral health at April 2012, worldwide 60 to 90 percent of school children and nearly 100 percent of adults experienced dental caries [1]. A significant general reduction in caries lesions has been noted in the United States in the last several decades with the increased availability of fluoride in public water supply, tooth paste and mouth rinse [1]. The greatest reduction in caries has been noted in smooth tooth surfaces. This type of interproximal lesion can be more easily identified by radiographic techniques [2]. Occlusal lesions have become the largest proportion of the total caries burden [3]. Clinical standards for diagnosing carious lesions of teeth include visual inspection of tooth surface (color evaluation, translucency), analysis of radiographic images, evaluation of dental surface porosity or hardness; visually or using tactile sense [3]. The research of designing diagnostic tools in caries has been at peak for the last decade. However, no such study has been done to detect and score caries with the use of optical images. The current diagnostic methods have a high false positive and false negative rate when diagnosing caries on occlusal surfaces, especially when using radiography which is the most accepted diagnostic method

Leila Ghaedi is student at Virginia Commonwealth University, Richmond, VA 23284 USA (phone: 804-938-8443; fax: 804-827-0006; Email: ghaedil@vcu.edu).

Riki Gottlieb, David C. Sarrett and Rosalyn H. Hargraves are faculty of Virginia Commonwealth University.

Kayvan Najarian and Ashwin Belle are with University of Michigan.

Amid Ismail is faculty of Temple University.

for caries detection [3,6]. ICDAS integrated several criterias into one standard for caries detection [8]. Studies assessed reproducibility and accuracy in the detection and assessment of occlusal caries in extracted teeth using ICDAS with histology as the 'gold standard' and moreover, better accuracy was achieved in detecting early lesions [9]. Existing technologies for caries diagnosis include devices based on laser fluorescence (LF) or infrared (IR) laser fluorescence, referred to as quantitative laser or light fluorescence (QLF). Other technologies include electrical conductance measurements (ECM), direct digital radiography, Digital Imaging Fiber-Optic Trans-Illumination (DIFOTI), simple Fiber Optic Trans-Illumination (FOTI), LED-based caries detector and less popular fluorescence spectrophotometer [3, 6-9]. These technologies have relatively high prices. Data shows varying degrees of sensitivity and specificity for in vitro and in vivo studies [3, 7, 10-11]. This study has been designed to incorporate digital images acquired from a variety of sources including off-the-shelf commercially available intra-oral cameras which are inexpensive in comparison to other dental imaging modalities.

The objective of this research is to design an automated system to detect and score dental caries. The input of the system is an optical image of the occlusal tooth surface which has been taken with an intraoral camera and the output of the system is an ICDAS score which quantifies the presence and severity of caries on that tooth surface. ICDAS scores are described as follows, 0: sound tooth, 1: first visual change in enamel, 2: distinct visual change in enamel, 3: localized enamel breakdown because of caries with no visible dentin or underlying shadow, 4: underlying dark shadow from dentin with or without localized enamel breakdown, 5: distinct cavity with visible dentin, 6: extensive distinct cavity with visible dentin [8]. Solving this particular problem needs several stages: (1) Create a segmentation method, to effectively segment the tooth surface images into background, regular tooth surface and irregular regions according to the guidelines for clinical caries detection. (2) Extract a set of features from the tooth image. The proposed method utilizes the extracted features and selects only the predominant features through a multi-stage feature selection process in order to automatically score the caries. (3) A modified classification technique is designed which classifies the features extracted from tooth images into the clinical scores. For computing the classification model, an ensemble classifier has been developed which essentially encompasses four different classification methods.

The rest of this paper is organized as follows. Section II describes the methodology, section III gives the experiment and data details, section IV gives the results a

nd discussions and section V gives the conclusion.

## II. METHODOLOGY

The proposed computational method analyzes photographs captured by digital cameras and produces predictions as to the existence and the severity of caries. The method first segments the tooth image into background, healthy enamel surface, and any irregular regions. Irregular regions, for this study, are the regions of interest for dentists, which show a variation in color, translucency and porosity. The irregular regions are defined by spatial statistics as well as texture analysis. Adding texture information empowers the system to not only identify visible changes in the enamel, but also the textural changes which are not visible and usually are detectable only by tactile examination. These features are then used to detect the existence and severity of caries in the identified irregular regions. The proposed method includes four major steps: Pre-Processing, Image Segmentation, Feature Extraction, and Feature Selection and Classification.

### A. Pre-Processing

Although the original image of the tooth surface is in color, other than feature extraction, most of image processing steps have been performed on the gray level interpolation of the original image. A histogram based contrast enhancement is applied to the gray level image to improve performance in the subsequent the image processing steps. The gray level transformation function,  $T(r_k)$  is given by equation 1.

$$S_k = T(r_k) = \sum_{j=0}^k P_r(r_j) = \sum_{j=0}^k \frac{n_j}{n} \quad (1)$$

Where,  $0 \leq r_k \leq 1$  and  $k=0,1,\dots,L-1$  and  $P_r(r_j)=n_j/n$  is the probability density function of the input image level  $j$ ,  $n$  is the total number of pixels in the input image and  $n_j$  is the number of pixels at level  $j$  [12]. The resulting image is used for image segmentation.

### B. Image Segmentation

Segmentation is performed in two stages. In the first stage the tooth surface is segmented with application of a region growing method and Circular Hough Transform (CHT). The second step identifies the irregular regions within the tooth boundaries by applying morphology operators to assess texture.

In the first step, CHT [13-14] is used to find a circle which roughly encompasses the tooth boundary. This technique has been chosen because of the semi-circle shape of the tooth's occlusal surface. The CHT identifies the circular shapes in the image, where each circle is defined by parameter triples  $(a, b, R)$ , where  $(a, b)$  is the center and  $R$  the radius. A threshold function is then applied to the radii of the set of identified circles, where circles with radius less than the threshold are removed and the mean values of the remaining circle parameters  $(a_{\text{mean}}, b_{\text{mean}}, R_{\text{mean}})$  are selected as the starting point for the region growing method [15]. The region growing method is used to approximate the outline of the tooth allowing the creation of a background mask which differentiates the tooth from the background.

To start irregular region detection, the background mask created from the previous step is applied to the color image. The resulting Tooth Boundary Color Image (TBCI) is used for the subsequent steps in which the irregular regions are identified.

The mean value of the first component of the RGB color space (Mean of RED) of TBCI is calculated then a black and white mask is generated by applying the Mean of RED threshold value to the TBCI. This black and white mask is then convolved by a low pass filter of size  $9 \times 9$  to smooth and reduce the number of connected components. Morphological operations are applied to remove the spurious edges and objects with an area smaller than  $3 \times 3$  squares. The resulting black and white mask is then applied to the color image. Haar Wavelet transform is then applied to the output in order to reconstruct the image using only the approximation coefficient matrix. A single-level discrete two-dimensional Haar wavelet transform is used in this study for texture analysis. The Haar wavelet is selected as the mother wavelet because of its discontinuity and intrinsic ability to accentuate transitions between gray levels. The Haar mother wavelet's function  $\psi(t)$  is described in equation 2 and its scaling function  $\Phi(t)$  is described in equation 3 [16].

$$\Psi(t) = \begin{cases} 1 & 0 \leq t \leq \frac{1}{2} \\ -1 & \frac{1}{2} \leq t \leq 1 \\ 0 & \text{otherwise} \end{cases} \quad (2)$$

$$\psi_{n,k}(t) = 2^{\frac{n}{2}} \psi(2^n t - k), t \in \mathbf{R} \quad (3)$$

Then the mean value ( $\alpha$ ) and standard deviation ( $\beta$ ) of this image is calculated and  $\alpha + \beta$  is used as a threshold, wherein the binary mask is created by selecting the pixels that have gray levels greater than threshold. Morphological operations are applied again to the binary mask to remove any objects smaller than  $3 \times 3$  squares. The resulting black and white mask identifies the irregular regions.

### C. Feature Extraction

A  $10 \times 10$  window is used to calculate features from the irregular regions and the entire enamel surface. Experimental testing with different window sizes ranging from  $7 \times 7$  to  $12 \times 12$  revealed that the window size of  $10 \times 10$  worked best for this application. At the end of the computation the proposed system extracts 77 region-based and pixel-based features from both enamel (as control) as well as the irregular regions separately based on color space using both wavelet and Fourier transforms. A number of these features are described next.

Entropy is a statistical measure of randomness that can be used to characterize the texture of the input image. Equation 4 shows the entropy, where  $p$  contains the histogram counts.

$$\text{Entropy} = - \sum_{i=1}^N \sum_{j=1}^M p(i,j) \log(p(i,j)) \quad (4)$$

The mean of matrix elements in a  $10 \times 10$  window is calculated as described in equation 5.

$$\text{Mean of matrix elements} = \frac{1}{100} \sum_{i=1}^{10} \sum_{j=1}^{10} f(i,j) \quad (5)$$

An image gradient, which described in equation 6 is a directional change in the intensity or color in the image.

$$\text{Gradient} = \Delta f = \frac{\Delta f}{\Delta x} + \frac{\Delta f}{\Delta y} \quad (6)$$

Table 1 describes how the features are created in both local and global levels and also how their statistical measures create the final feature pool for each image. Subscript 2 implies that the feature was computed inside each local 10 x 10 window and subscript 1 implies that the feature was computed on a global level across the image. The table shows 38 possible features which are calculated for both the tooth surface excluding irregular regions and as well as the irregular regions computed separately; this finally gives us 76 features. A final feature that is also included to the feature pool is the ratio of the total area of irregular regions to the total tooth region.

	A	B	C	D	E	F	G
Mean <sub>1</sub> (Mean <sub>2</sub> )	X	X	X	X	X	X	X
Std <sub>1</sub> (Mean <sub>2</sub> )	X	X	X	X			
Median <sub>1</sub> (Mean <sub>2</sub> )	X	X	X	X			
Maximum <sub>1</sub> (Mean <sub>2</sub> )	X	X	X	X			
Maximum <sub>1</sub> (Gradient <sub>2</sub> )	X	X	X	X			
Mean <sub>1</sub> (Maximum <sub>2</sub> )	X	X	X	X			
Mean <sub>1</sub> (Minimum <sub>2</sub> )	X	X	X	X			
Entropy <sub>1</sub>	X	X	X	X	X	X	X

Table 1. Feature Extraction at 10 by 10 windows level and the whole image level. A: First Component of Color Space (RED), B: Second Component of Color Space (GREEN), C: First Component of Color Space (BLUE), D: Gray Scale Image, E: Single-level Haar Wavelet Decomposition, F: Second-level Haar Wavelet Decomposition, G: Fourier Transform

### C. Feature Selection and Classification

Since attempting to classify the small number of available data into 7 different classes based on the ICDAS scale, the ICDAS scores in our study were grouped into three overview classes; Sound occlusal (ICDAS Score 0), Initial caries (ICDAS Score 1 or 2), Moderate to severe caries (ICDAS Score 3 to 6) [19]. In our previous work, the seven ICDAS classes were dichotomized into two classes, which resulted in 80.8% accuracy for automatic detection of two classes across 72 images [20]. Other studies also re-categorized ICDAS scores to fewer categories than the initial 7 scores [7, 21, 13-14, 19-20]. A heuristic super classifier method is applied to select only high ranking features thereby reducing the feature space for the development of the classifier model [22]. Feature ranking was performed using the information-gain ratio method; wherein the features are ranked according to their contribution to distinguishing the categories. An extensive search was performed to find the best subset of features and the best classifier. In this search, highest ranked feature subsets starting from 5 top ranked features all the way to the entire feature set were comprehensively tested against the classifiers to determine where the output accuracy peaked. It was identified that the subset of the top 12 ranked features provided the highest classification accuracy. During this exhaustive search, the different classifiers as well as their parameters were optimized to identify the best setup for obtaining the most accurate classification model. Five was chosen as the minimum number of selected features because any less than that did not provide sufficient information to classify items into three classes. The super classifier method encompasses four classification methods to perform the classification task which includes C4.5 decision tree [23], Super Vector Machine (SVM) [24], Random Forest classifier [25] and Artificial Neural Network classifier [26].

These methods have been popular in the development of medical decision support systems. To avoid possibilities of over fitting the model was validated using a non-stratified ten-fold cross validation system.

### III. EXPERIMENT AND DATA

The data used in this study consist of two sets of color images; while both sets contain images taken from extracted human teeth, they have different levels of resolution and background. The first set includes 72 images of size 1440×2160×3 with a blue background these were provided by a previous cariology study conducted in 2001 [17]. The second set consists of 16 images of size 768×1024×3 with a black background. These were collected, analyzed and scored at VCU School of Dentistry during the VCU-ICDAS Training Workshop in 2011 [18]. All the images show the occlusal surface of an extracted tooth, one image per tooth surface. All images were scored by ICDAS experts. The combined dataset consists of images of 19 premolar and 69 molar teeth with different stages of caries.

### IV. RESULT AND DISCUSSION

The output of super-classifier was a Random Forest Classifier with 12 high ranked features. Three-classes, classification resulted in 86.3% of accuracy, 98.3% of specificity, and 83.0% of sensitivity, with a Kappa coefficient of 71%. Standard deviation of (accuracy= 1.8%, specificity=1.9%, sensitivity=1.7%) and Analysis of variance (ANOVA) on selected features regarding the output categories, showed that the selected features were statistically significant (p-value=0.05).

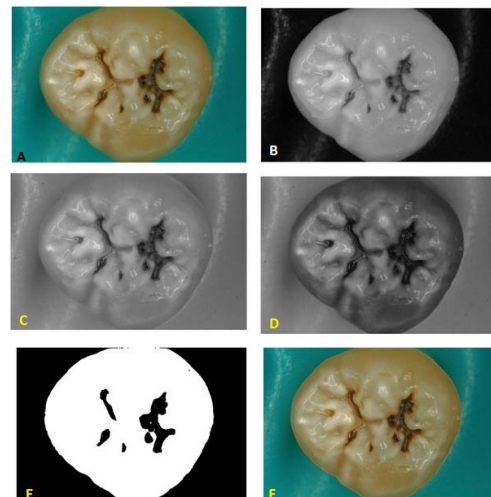


Figure 1: Image number 24 with a ICDAS score of 4 (Underlying Dentin Shadow) A: Original Image, B: Red Component, C: Green Component, D: Blue Component, E: Segmentation Result Black and White Mask, F: Segmentation Result on color Image

	0PSS	1-2PSS	3-6PSS	Sum of
0ICDAS	9	3	0	12
1-2ICDAS	2	43	2	47
3-6ICDAS	0	5	24	29
Sum of Columns	11	51	26	-

Table 2: Confusion Matrix for the proposed system score (PSS), comparing it to the gold standard which is the ICDAS scores. PSS has been generated by the system and where ICDAS experts' scores are the scores that ICDAS experts assigned to each tooth after examining the extracted tooth as well as looking at the images of occlusal surface.

## V. CONCLUSION

We developed and tested an automated system to detect and score caries lesions based on occlusal tooth surface images, using ICDAS as the standard. In this study, an automated and user friendly system has been proposed that eliminates the need for manual land-marking while using advanced feature extraction methods leading to a more reliable system for detection of early caries lesions. The results support further investigation of the use of optical images for clinical caries diagnosis.

This study's limitations include: 1) small number of images for each of the seven ICDAS categories. 2) Unbalanced number of image samples in each of the seven ICDAS categories. 3) Based on extensive findings of other studies, histological verification of the diagnosis has not been performed. 4) Images were of extracted teeth. A continued study would be required for testing and validating the system's performance on larger datasets and *in vivo* samples.

The designed system may provide an advantage over existing systems, since it does not require expensive imaging sensors and/or external hardware. Olsen et al. [27] described a system that used photographs captured by a digital camera to develop an Active Shape Modeling Algorithm for image segmentation which required manual land-marking and guidance. Jablonski-Momeni et al. [11] assessed the performance of LF, an LF pen, and fluorescence camera (FC) in detecting occlusal caries (Carious versus Non-Cariou) by using histological information as gold standard described specificity and sensitivity levels of 100% and 85% for LF, 80% and 89% for LF pen, and 80% and 74% for FC respectively [11]. These are comparable to the specificity and sensitivity of 86.2% and 96.6% achieved in this study when classifying into two classes but not three. The proposed system's performance is better than LF pen and FC and almost similar to LF.

## ACKNOWLEDGMENT

The authors acknowledge Dr. Andrea Zandona, Director, Early Caries Research Program, Indiana University School of Dentistry, for her contribution in data collection.

## REFERENCES

- [1] <http://www.who.int/mediacentre/factsheets/fs318/en/>
- [2] Caries Annual Report - NIDCR/CDC Dental, Oral and Craniofacial Data Resource Center (DRC), [http://drc.hhs.gov/report/1\\_3.htm](http://drc.hhs.gov/report/1_3.htm) accessed on 8/29/13.
- [3] A.F. Zandona, D.T. Zero, Diagnostic tools for early caries detection, *The Journal of the American Dental Association* 137 (12) (2006) 1675-1684.
- [4] A.I. Ismail, Visual and Visuo-tactile Detection of Dental Caries, *Journal of Dental Research* 83 (2004) C56-C66.
- [5] B. Senel, K. Kamburoglu, O. Ucok, S.P. Yuksel, T. Ozen, H. Avsever, Diagnostic accuracy of different imaging modalities in detection of proximal caries, *Dentomaxillofacialradiology* 39 (8) (2010) 501-511.
- [6] G.K. Rochlen, M.S. Wolff, Technological advances in caries diagnosis, *Dental clinics of North America* 55 (3) (2011) 441-452.
- [7] M.B. Diniz, T. Boldieri, J.A. Rodrigues, L. Santos-Pinto, A. Lussi, R.C. Cordeiro, The performance of conventional and fluorescence-based methods for occlusal caries detection: an *in vivo* study with histologic validation, *Journal of the American Dental Association* 143 (4) (2012) 339-350.
- [8] International Caries Detection and Assessment System (ICDAS) Coordinating Committee, *Criteria Manual International Caries Detection and Assessment System (ICDAS II)*, (2009).
- [9] O. Samek, H.H. Telle, D.C.S. Beddows, Laser-induced breakdown spectroscopy: a tool for real-time, *in vitro* and *in vivo* identification of carious teeth, *BMC Oral Health* 1 (2001) 1-1.
- [10] A.M. Aktan, M.A. Cebe, M.E. Ciftci, E.S. Karaarslan, A novel LED-based device for occlusal caries detection, *Lasers in Medical Science*. 27 (2012) 1-7.
- [11] A. Jablonski-Momeni, D.N. Ricketts, S. Rolfsen, R. Stoll, M. Heinzl-Gutenbrunner, V. Stachniss, K. Pieper, Performance of laser fluorescence at tooth surface and histological section, *Lasers in Medical Science* 26 (2) (2011) 171-178.
- [12] V. Agarwal. Analysis of Histogram Equalization in Image Preprocessing. *BIOINFO Human-Computer Interaction*. 1(1):4-7, 2011.
- [13] R.O. Duda, P.E. Hart, Use of the Hough Transformation to Detect Lines and Curves in Pictures, *Communication of the ACM* 15 (1) (1972) 11-15.
- [14] M. Rizon, H. Yazid, P. Saad, A.Y.M. Shakkaf, A.R. Saad, S. Masanori, S. Yaccob, M.R. Mamat, M. Karthigayan, Object detection Using Circular Hough Transform, *American Journal of Applied Sciences* 2 (12) (2005) 1606-1609.
- [15] R. Adams and L. Bischof, Seeded Region Growing, *IEEE Transaction on Pattern Analysis and Machine Intelligence* 16 (6) (1994)641-647.
- [16] I. Daubechies, Ten lectures on wavelets, CBMS-NSF conference series in applied mathematics, SIAM Ed (1992).
- [17] A. Jablonski-Momeni, V. Stachniss, D.N. Ricketts, M. Heinzl-Gutenbrunner, K. Pieper, Reproducibility and accuracy of the ICDAS-II for detection of occlusal caries *in vitro*, *Caries Research* 42 (2) (2008) 79-87.
- [18] Dean's blog, Virginia Commonwealth University, School of Dentistry, <http://wp.vcu.edu/dentistrydean/2012/01/07/icdas-training-and-caries-management-strategies/>, accessed on 8/29/2013.
- [19] A.I. Ismail, M. Tellez, N.B. Pitts, K.R. Ekstrand, D. Ricketts, C. Longbottom, H. Eggertsson, C. Deery, J. Fisher, D.A. Young, J.D.B. Featherstone, R.W. Evans, G.G. Zeller, D. Zero, S. Martignon, M. Fontana, A. Zandona, Caries management pathways preserve dental tissues and promote oral health, *Community Dent Oral Epidemiol* 41 (2013) e12-e40.
- [20] L. Ghaedi, R. Gottlieb, K. Najarian, Towards An Automated Caries Detection System Using Intra-Oral Photographs, AADR Annual Meeting Tampa, Florida, March 2012 Proceeding (2012).
- [21] M.M. Braga, M.S. de Benedetto, J.C. Imparato, F.M. Mendes, New methodology to assess activity status of occlusal caries in primary teeth using laser fluorescence device, *Journal of Biomedical Optics* 15 (4) (2010) 047005.
- [22] A. Belle, M. Pfaffenberger, R. H. Hargraves and K. Najarian. An Automated Decision Making System for Detecting Loss of Attention in Individuals Using Real Time Processing of Electroencephalogram. *Biosignal Interpretation-7<sup>th</sup> International Workshop*, 2012.
- [23] J.R. Quinlan, J. Ross, C4.5: programs for machine learning, Morgan Kaufmann Publishers (1994).
- [24] H.E. Strassler, L.G. Sensi, Least Square Support Vector Machine Classifiers, *Neural Processing letters* 9 (1999) 293-300.
- [25] L. Breiman, Random Forests, *Machine Learning* 45 (2001) 5-32.
- [26] S. Dreiseutl, L. Ohno-Machado, Logistic regression and artificial neural network classification models: a methodology review, *Journal of Biomedical Informatics* 35(5) (2002) 352-359.
- [27] G.F. Olsen, S.S. Brilliant, D. Primeaux, K. Najarian, An Image-Processing Enabled Dental Caries Detection System, ICME International Conference on Complex Medical Engineering (2009).